

Saturation of intraband absorption and electron relaxation time in *n*-doped InAs/GaAs self-assembled quantum dots

S. Sauvage and P. Boucaud^{a)}

Institut d'Électronique Fondamentale, URA CNRS 22, Université Paris-Sud, 91405 Orsay, France

F. Glotin, R. Prazeres, and J.-M. Ortega

CLIO/LURE, Université Paris-Sud, 91405 Orsay, France

A. Lemaître, J.-M. Gérard, and V. Thierry-Fleg

Groupeement Scientifique CNET-CNRS, 196 Av. H. Ravera 92225 Bagneux, France

(Received 15 June 1998; accepted for publication 22 October 1998)

We have observed the saturation of intraband absorption in InAs/GaAs self-assembled quantum dots. The investigated *n*-doped self-assembled quantum dots exhibit an intraband absorption within the conduction band, which is peaked at an 8 μm wavelength. The saturation of the intraband absorption is achieved with an infrared pump delivered by a pulsed free-electron laser. The saturation of the transition is observed for an intensity around $\approx 0.6 \text{ MW cm}^{-2}$. The electron relaxation time under intraband excitation is measured by time-resolved pump-probe experiments. An electron relaxation time $T_1 \approx 3 \text{ ps}$ is reported. © 1998 American Institute of Physics. [S0003-6951(98)03852-2]

The relaxation time between excited levels in semiconductor self-assembled quantum dots is predicted to be several order of magnitude larger than in two-dimensional (2D) systems due to the so-called phonon bottleneck.¹ Time-resolved photoluminescence measurements have effectively shown that the relaxation times are longer in quantum dots than in quantum wells, typically, of the order of 20 ps.^{2,3} Although the phonon bottleneck is not as marked as predicted, the observed reduction of the electron relaxation rate is a direct consequence of the three-dimensional (3D) confinement potential. If the energy separation between the confined states exceeds the phonon energy, the relaxation can only proceed by multiphonon emission or Auger-like relaxation mechanisms.⁴⁻⁶ The reduction of the relaxation should have direct consequences for optoelectronic devices, in particular, for the operation of quantum dot infrared photodetectors. By analogy with quantum well infrared photodetectors, which are based on intersubband transitions, quantum dot infrared photodetectors relying on intraband transitions can be realized. One key parameter which controls the performances of the quantum well infrared photodetectors is the capture and the relaxation of the carriers from the barrier into the well. In quantum wells and for energies larger than the (LO) phonon energy, this relaxation time is around 1 ps due to the efficient LO-phonon scattering.⁷ An increase of the relaxation time should improve the detector performances, in particular, the temperature of background-limited infrared performance. The predicted reduced relaxation in quantum dots has, therefore, motivated the study of quantum dot based infrared photodetectors. Reports of midinfrared photoconductivity have been published by several groups.^{8,9} However, the data were not quantitative and the electron relaxation time could not be deduced from their measurements.

We have recently shown that *n*-doped InAs/GaAs self-

assembled quantum dots exhibit *z*-polarized intraband absorption in the 8–12 μm wavelength range.¹⁰ This absorption was attributed to the intraband transition between the bound dot ground state to the continuum states in the wetting layer. The energy maximum of the intraband transition is adjustable as a function of the quantum dot size. In this letter, we first show that the intraband absorption can be saturated at high pump intensity using a free-electron laser. In a second part, the measurement of the electron relaxation time by time-resolved pump-probe experiments is reported. We have measured an electron relaxation time $T_1 \approx 3 \text{ ps}$ when the intraband absorption is bleached.

The sample consists of 20 InAs/GaAs quantum dot layers separated by 50 nm thick GaAs barriers. The quantum dots were grown by molecular beam epitaxy. The dots have a lens-shaped geometry and the density is around $9 \times 10^{10} \text{ cm}^{-2}$, as measured by plan-view and cross-sectional electronic transmission microscopy. The quantum dots are modulation doped with a silicon δ doping layer 2 nm above the InAs layer. The bidimensional carrier density of the planar doping is $6 \times 10^{10} \text{ cm}^{-2}$. The 20 layers are embedded in a midinfrared waveguide.¹¹ The waveguide consists of a 5.5 μm thick GaAs core grown on a 5 μm thick $\text{Al}_{0.9}\text{Ga}_{0.1}\text{As}$ cladding layer. The quantum dots are inserted in the GaAs core. The whole structure is grown on a n^+ -doped GaAs substrate. A similar waveguide with undoped quantum dots has been grown as a reference. The saturation absorption measurements were performed at room temperature with a pump beam provided by a free-electron laser. The free-electron laser delivers macropulses with a 10 μs duration at a repetition rate of 25 Hz. Each macropulse consists of picosecond micropulses with a time separation of 32 ns. For saturation measurements, the waveguide length was 5 mm.

The quantum dot energy levels in the conduction band have been calculated by solving the three-dimensional Schrödinger equation in the effective-mass approximation.¹²

^{a)}Electronic mail: phill@ief.u-psud.fr

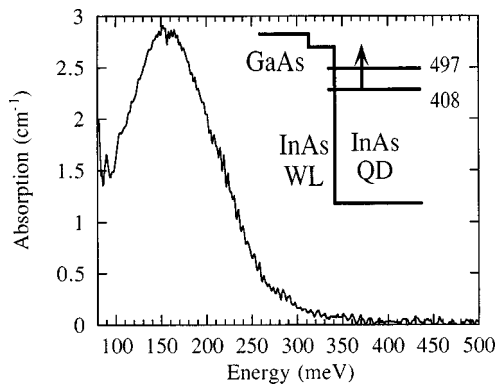


FIG. 1. Room-temperature midinfrared linear absorption spectrum of n -doped InAs/GaAs self-assembled quantum dots. The absorption is measured in waveguide geometry. The inset shows the schematic conduction-band-energy diagram of the lens-shaped InAs/GaAs quantum dots (QD). WL stands for the wetting layer. The calculated energy levels (meV) are referred to the bottom of the InAs conduction band. The arrow shows the z -polarized intraband absorption.

The numerical calculations were performed for a lens-shaped dot geometry with a height of 2.2 nm and a base diameter of 22 nm. The strain-induced modification of the effective mass was accounted for by taking an isotropic effective mass of $0.04 m_0$ in the InAs layer, where m_0 is the free-electron mass.¹³ The energy diagram of the quantum dot in the conduction band is depicted in the inset of Fig. 1. The energy of the ground level is 408 meV above the InAs band edge. The first excited level is doubly degenerate and lies 89 meV above the ground state. The next levels are hybridized with the InAs wetting layer states. The energy of the wetting layer is found at 560 meV above the InAs band edge while the GaAs barrier lies 600 meV above InAs. Note that a slight increase of the base diameter leads to a second confined state just below the InAs wetting layer. For intraband measurements and assuming that only the ground state is populated, one expects, therefore, an intraband absorption polarized in the layer plane at around 89 meV ($\approx 13.9 \mu\text{m}$ wavelength) and an intraband transition at around 152 meV ($\approx 8.15 \mu\text{m}$ wavelength) with a dipole along the z growth axis (i.e., TM polarization).

Figure 1 shows the linear absorption of the sample in TM polarization. The measurement was performed with a Fourier transform infrared spectrometer coupled to an infrared microscope. The transmission has been normalized by the transmission of the undoped reference waveguide. The absorption is maximum at 157 meV with an inhomogeneous broadening (half width at half maximum) ≈ 50 meV. This inhomogeneous broadening stems mainly from the size distribution of the dots. As predicted, the intraband transition corresponds to a bound-to-continuum transition. There is very good agreement between the calculated and measured intraband energies, but this agreement remains strongly dependent on the dot geometry. A weak monotonous absorption which increases towards low energy contributes also to the absorption. It is attributed to the residual free-carrier absorption of the carriers, which are not transferred into the dots. Note that the spectrum is very similar to the one reported earlier in the multipass geometry.¹⁰ In waveguide geometry, the absorption cross section of one dot layer can be

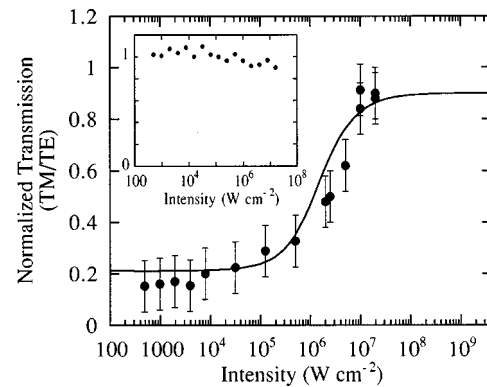


FIG. 2. Room-temperature waveguide transmission for the n -doped sample (dots) as a function of the pump intensity. The normalized transmission is given by the ratio of transmission in TM and TE polarizations. The inset shows the same ratio in the undoped waveguide sample. The pump wavelength is set at $8 \mu\text{m}$. The full curve is a fit which accounts for the propagation and attenuation of the pump beam.

deduced from the expression of the absorption coefficient per unit length (1)

$$\alpha = \sum_i \sigma n_{2D} \frac{\xi_i^2}{\int \xi^2 dy}, \quad (1)$$

where σ is the absorption cross section, n_{2D} the bidimensional carrier density, and ξ_i the amplitude of the electric field of the TM mode for the i th layer plane. The summation is over the 20 layer planes and the integral is performed over the extension of the TM mode. Assuming that about half the carriers are transferred in the quantum dots, i.e., $n_{2D} \approx 3 \times 10^{10} \text{ cm}^{-2}$, one finds $\sigma \approx 1 \times 10^{-15} \text{ cm}^2$. The absorption cross section is slightly lower than the one reported earlier.¹⁰ The discrepancy is likely related to a probable overestimation of the electronic charge which is effectively transferred for this sample at room temperature into the dots. A weak absorption is also observed in TE polarization with a maximum around 200 meV.¹²

Variation of the transmission at the $8 \mu\text{m}$ wavelength as a function of the pump intensity coupled in the waveguide is shown in Fig. 2. The transmission is normalized by the transmission in TE polarization. The transmission of the undoped sample is also shown as a reference. For the undoped waveguide, the transmission remains constant in the investigated intensity range. On the contrary, in the case of the n -doped sample, the transmission increases above 10 kW cm^{-2} and reaches a maximum at 10 MW cm^{-2} . At this intensity, the intraband absorption is almost completely bleached. The normalized transmission saturates at around 0.9, which corresponds to the ratio of the TM/TE transmission in the presence of residual free-carrier absorption. The free-carrier absorption does not saturate in the investigated energy range. We underline that, like in hole burning experiments in the presence of inhomogeneous broadening, only a fraction of quantum dots have their intraband absorption bleached. The variation of transmission has been modeled by taking into account the propagation along the 5 mm waveguide and the saturation of the absorption. Due to the attenuation of the pump beam, the absorption is not saturated identically along the penetration depth. This effect leads to an *apparent* higher

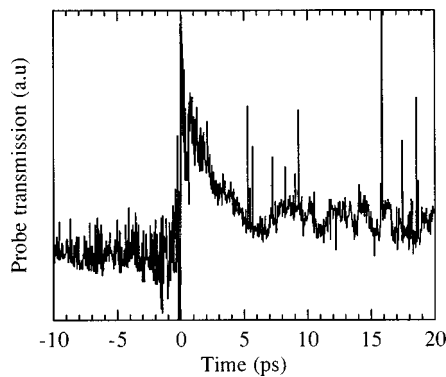


FIG. 3. Room-temperature probe transmission in TE polarization vs the time delay between the pump and probe. The pump intensity is $\approx 10 \text{ MW cm}^{-2}$. The pump and probe wavelengths are $8 \mu\text{m}$.

saturation intensity. The result is shown as a full line in Fig. 2. This fitting procedure gives a saturation intensity $I_s \approx 600 \text{ kW cm}^{-2}$.

The estimation of the relaxation time from the saturation intensity is not straightforward in the present experiment. First, this estimation is directly dependent on the intensity coupled in the waveguide, which can be overestimated. Second, one would expect a much lower saturation intensity for the quantum dots. Indeed, the intraband transition of an individual quantum dot is expected to be lifetime broadened, as a consequence of the δ -like density of states: any inelastic dephasing process corresponds to the scattering of the carriers from one level to another and is thus associated with the lifetime of the carriers. The coherence time, which is proportional to the relaxation time ($T_2 = 2T_1$),¹⁴ is therefore, expected to be rather long in quantum dots. Typically, a coherence time of 6 ps should lead to narrow linewidths ($\approx 100 \mu\text{eV}$) for the intraband transitions and to saturation intensities which are of the order of 10 kW cm^{-2} rather than 600 kW cm^{-2} . In the present experiment, the quantum dots are excited by optical pulses with pulse duration $\approx 2.5 \text{ ps}$, which is, therefore, lower than an expected typical coherence lifetime. As a consequence, the population does not have time to reach steady state.¹⁵ This feature explains that it is, therefore, necessary to pump with a much higher intensity than the saturation intensity to achieve bleaching of the intraband absorption.

In order to measure the electron relaxation time, we have performed time-resolved pump-probe measurements. The experiment was performed with a high pump intensity as reported above and with a 1 ps pulse duration. The pump was set in TM polarization while the probe was set at 45° between TE and TM polarization. We have measured the variation of transmission in TE polarization as a function of the time delay between the pump and probe. The TE polarization was chosen for the transmission in order to have a high rejection of the pump beam. The probe transmission versus the time delay between the pump and probe is reported in Fig. 3. As seen, the transmission is modified when the pump and probe are coincident. The transmission recovers its value ($1/e$ of maximum) after $\approx 3 \text{ ps}$.¹⁶ This measurement gives a direct value of the electron relaxation time T_1 after an excitation at the $8 \mu\text{m}$ wavelength. Note that there is no long-lived component in Fig. 3. The slightly higher value

of the transmission at large time delay only results from the fluctuation of the average power of the free-electron laser during the accumulation of the scan. We can first observe that the 3 ps relaxation time is longer than the one measured by saturation spectroscopy of intersubband transitions in quantum wells or similar time-resolved measurements (0.25–1 ps).^{17,18} The 3 ps relaxation time indicates that the relaxation is less efficient in 3D confined systems than in 2D confined systems. However, this value remains short if it is compared to the one reported by time-resolved photoluminescence experiments at low temperature.^{2,3} In *n*-doped (i.e., hole-free) quantum dots, Auger-like relaxation mechanisms involving electrons and holes can be ruled out. In our experiment, multiphonon relaxation mechanisms or Auger-like relaxation involving only electrons¹⁹ appear, however, to be relatively efficient. In Ref. 19, Uskov *et al.* have shown that carrier relaxation by Coulomb interaction with two-dimensional carriers can lead to ps recombination times. The presence of carriers in the 2D wetting layer under high pump intensity could explain the observed relatively fast relaxation. It is interesting to note that a similar electron relaxation time (5.2 ps) has been recently reported using time-resolved differential transmission spectroscopy experiments in InGaAs quantum dots.²⁰

This work was supported by DGA under Contract No. 97062/DSP.

¹H. Benisty, C. M. Sotomayor-Torres, and C. Weisbuch, *Phys. Rev. B* **44**, 10945 (1991).

²J.-M. Gérard, in *Confined Electrons and Photons*, edited by E. Burstein and C. Weisbuch (Plenum, New York, 1995).

³B. Ohnesorge, M. Albrecht, J. Oshinowo, A. Forchel, and Y. Arakawa, *Phys. Rev. B* **54**, 11532 (1996).

⁴T. Inoshita and H. Sakaki, *Phys. Rev. B* **46**, 7260 (1992).

⁵U. Bockelmann and T. Egeler, *Phys. Rev. B* **46**, 15574 (1992).

⁶A. L. Efros, V. A. Kharchenko, and M. Rosen, *Solid State Commun.* **93**, 281 (1995).

⁷M. C. Tatham, J. F. Ryan, and C. T. Foxon, *Phys. Rev. Lett.* **63**, 1637 (1989).

⁸J. Phillips, K. Kamath, and P. Bhattacharya, *Appl. Phys. Lett.* **72**, 2020 (1998).

⁹S. Maimon, E. Finkman, G. Bahir, S. E. Schacham, J. M. Garcia, and P. M. Petroff, *Appl. Phys. Lett.* **73**, 2003 (1998).

¹⁰S. Sauvage, P. Boucaud, F. H. Julien, J. M. Gérard, and V. Thierry-Mieg, *Appl. Phys. Lett.* **71**, 2785 (1997).

¹¹O. Gauthier-Lafaye, P. Boucaud, F. H. Julien, S. Sauvage, S. Cabaret, J.-M. Lourtioz, V. Thierry-Mieg, and R. Planel, *Appl. Phys. Lett.* **71**, 3619 (1997).

¹²S. Sauvage, P. Boucaud, J.-M. Gérard, and V. Thierry-Mieg, *Phys. Rev. B* **58**, 10562 (1998).

¹³M. A. Cusack, P. R. Briddon, and M. Jaros, *Phys. Rev. B* **56**, 4047 (1997).

¹⁴K. L. Campmann, H. Schmidt, A. Imamoglu, and A. C. Gossard, *Appl. Phys. Lett.* **69**, 2554 (1996).

¹⁵T. A. DeTemple, L. A. Bahler, and J. Osmundsen, *Phys. Rev. B* **24**, 1950 (1981).

¹⁶A similar relaxation time of 1.5 ps has also been measured for a bound-to-bound intraband transition in the valence band.

¹⁷J. Y. Duboz, E. Costard, E. Rosencher, P. Bois, J. Nagle, J. M. Berset, D. Jaroszynski, and J. M. Ortega, *J. Appl. Phys.* **77**, 6492 (1995).

¹⁸P. Boucaud, F. H. Julien, R. Prazeres, J. M. Ortega, V. Berger, J. Nagle, and J. P. Leburton, *Electron. Lett.* **32**, 2357 (1996).

¹⁹A. V. Uskov, F. Adler, H. Schweizer, and M. H. Pilkuhn, *J. Appl. Phys.* **81**, 7895 (1997).

²⁰T. S. Sosnowski, T. B. Norris, H. Jiang, J. Singh, K. Kamath, and P. Bhattacharya, *Phys. Rev. B* **57**, R9423 (1998).